https://doi.org/10.5194/essd-2022-68
Preprint. Discussion started: 4 March 2022

Microwave radiometry experiment for snow in Altay China: in situ time series of data for electromagnetic and physical features of snow pack and environment

Liyun Dai[1], Tao Che[1,2]*, Yang Zhang[1], Zhiguo Ren[1, 3], Junlei Tan[1], Meerzhan Akynbekkyzy[1], Lin Xiao[1], Shengnan Zhou[1], Yuna Yan[3], Yan Liu[4], Hongyi Li[1], Lifu Wang[5]

[1]Key Laboratory of Remote Sensing of Gansu Province, Heihe Remote Sensing Experimental Research Station, Northwest Institute of Eco-Environment and Resources, Chinese Academy of Sciences, Lanzhou, 730000, China.
[2]Center for Excellence in Tibetan Plateau Earth Sciences, Chinese Academy of Sciences, Beijing, 100101, China.
[3]University of Chinese Academy of Sciences, Beijing, 1000101, China. yunayan2008@163.com
[4] Institute of Desert Meteorology, China Meteorological Administration, Urumqi, 830002, China
[5]Altay National Reference Meteorological station, China Meteorological Administration, Altay, 836500, China.

Correspondence to: Tao Che (chetao@lzb.ac.cn)

Abstract. Snow depth is a key parameter in climatic and hydrological systems. Passive microwave remote sensing, snow process model and data assimilation are the main methods to estimate snow depth in large scale. The estimation accuracies strongly depend on input of snow parameters or characteristics. Because the evolving processes of snow parameters vary spatiotemporally, and are difficult to accurately simulate or observe, large uncertainties and inconsistence exist among existing snow depth products. Therefore, a comprehensive experiment is needed to understand the involution processes of snow characteristics and their influence on microwave radiation of snowpack, evaluating and improving the snow depth and SWE retrieval and simulation methods. An Integrated Microwave Radiometry Campaign for snow (IMCS) was conducted at the Altay National Reference Meteorological station (ANRMS) in Xinjiang, China, during snow season of 2015/2016. The campaign hosted a dual polarized microwave radiometer operating at L, K and Ka bands to provide minutely passive microwave observations of snow cover at a fixed site, daily manual snow pit measurements, ten-minute automatic 4-component radiation and layering snow temperatures, covering a whole snow season of 2015/2016. The measurements of meteorological and underlying soil parameters were requested from the ANRMS. This study provides a summary of the obtained data, detailing measurement protocols for microwave radiometry, in situ sow pit and station observation data. A brief analysis of the microwave signatures against snow parameters is presented. A consolidated dataset of observations, comprising the ground passive microwave brightness temperatures, in situ snow characteristics, 4-component radiation and weather parameters, was achieved in the National Tibetan Plateau Data Center, China. The dataset is unique in providing continuously daily snow pits data over a snow season at a fixed site and matched microwave brightness temperatures, radiation and meteorological data. The dataset is expected to serve for the evaluation and development of the microwave and optical radiative transfer models and snow evolution process models. The

https://doi.org/10.5194/essd-2022-68
Preprint. Discussion started: 4 March 2022

Open Access Earth System Science Data Discussions

consolidated data are available at https://data.tpdc.ac.cn/en/ (doi: 10.11888/Snow.tpdc.270886) (Dai, 2020).

Key words: Snow, Microwave radiometry, Snow pit, Experiment

1 Introduction

Seasonal snow cover plays a critical role in climate and hydrological systems (Cohen, 1994; Ding et al., 2020; Barnett et al., 2005; Immerzeel et al., 2010) by its high albedo, thermal insulation, fresh water reserves and its phase change process. Snow cover can be accurately identified by optical remote sensing. However, the snow surface albedo was controlled by snow characteristics (Aoki et al., 2003 and 2000), and the variations in snow characteristics cause the uncertainties of albedo estimation. Snow depth and snow water equivalent (SWE) are currently estimated using passive microwave in global and regional scales (Pullianen et al., 2020; Tedesco and Narvekar, 2010; Jiang et al., 2014; Che et al., 2008). Although several global and regional snow depth and SWE products have been released, large uncertainties exist in these products because of the spatio-temporal variations in snow characteristics (Xiao et al., 2020; Mortimer et al., 2020; Che et al., 2016; Dai et al., 2012). Therefore, the observation on electromagnetic and physical parameters of snowpack are necessary to improve understanding the electromagnetic radiation process of snowpack to enhance the estimation accuracy of snow surface albedo and snow depth.

To evaluate and improve snow depth and SWE retrieval methods from passive microwave remote sensing observations and to combine remote sensing technologies with modeling and data assimilation methods for producing the most accurate products, a few large or systematic experiments or campaigns had been conducted on electromagnetic and physical characteristics measurement of snow cover. The Cold Land Processes Field Experiment (CLPX) (https://nsidc.org/data/clpx/index.html) was one of the most well-known experiments, which was carried out from winter of 2002 to spring of 2003 in Colorado, USA (Cline et al., 2003). During the campaign, snow pits were collected at the February and March of 2002 and 2003 to coincide with the airborne and ground remote sensing observations. NASA SnowEx campaign (https://nsidc.org/data/snowex) was conducted in 2017 in Colorado to develop/test algorithms for measurement of SWE in forested and non-forested areas by providing multi-sensor observations of seasonally snow-covered landscapes (Brucker et al., 2017). The campaign is still ongoing and will be conducted in other areas with different snow conditions. In northern Canadian region, mobile sled-mounted microwave radiometers were deployed in forest, open and lake environments from November 2009 to April 2010 and snow characteristics within the footprints of radiometers were measured to improve understanding the influence of snow characteristics on brightness temperatures (Derksen et al., 2012; Roy et al., 2013). These microwave experiments were of mobile observation. In these experiments, there were multiple observation sites for different land cover, but relative short temporal range. The snow pit observations could be used for evaluating snow microwave emission model in different land cover (Tedesco and Kim, 2006; Royer et al., 2017), but they did not exhibit the involution of snow parameters.

In the Arctic region, the Nordic Snow Radar Experiment (NoSREx) campaign was conducted at a fixed field in Sodankylä, Finland, during 2009 ~ 2013 (Lemmetyinen et al., 2016). This experiment provided a continuous time series of active and passive microwave observations of snow cover at a representative location of the Arctic boreal forest area covering a whole winter season and matched snow pit observations were made weekly. In Asia, snow pit work of 3 or 4-day intervals was conducted

https://doi.org/10.5194/essd-2022-68
Preprint. Discussion started: 4 March 2022

simultaneously with radiation budget observations during winter of 1999/2000 and 2000/2001 to analyze the effects of snow physical parameters on albedo (Aoki et al., 2003). The NoSREx and Japan radiation experiments were of fixed field observation, which provided longer time series of data. These experiments were conducted in deep snow area, and the week-interval observation could reflect the general evolution process of snow characteristics, but might miss some details. Furthermore, in the area with snow cover duration within 4 months, the week-interval observation hardly depicts the change details.

To comprehensively understand the evolutions of snow characteristics and their influence on passive microwave brightness temperatures and radiation budget, an integrated experiment on snow was conducted during a whole snow season, in Altay, China. The experiment was designed to cover periods from snow-free conditions to eventual snow melt-off during 2015/2016. The microwave radiometry measurements at L, K and Ka bands for multiple angles were complemented by a dual-polarized microwave radiometer with 4-component radiation and daily in situ observations of snow, soil and atmospheric properties, using both manual and automated methods. The data of electromagnetic and physical parameters were further consolidated and organized to be easily read and utilized.

The dataset is unique in providing continuously daily snow pits data over a snow season at a fixed site and matched microwave brightness temperatures, radiation and meteorological data. In the next section, the experiment location, parameters, parameter measurement protocols are described; section 3 introduces the consolidated data which was released on the National Tibetan Plateau Data Center, China; section 4 presents content of brightness temperature, 4-component radiation, snow pit data, soil temperature and moisture, and meteorological data; section 5 discusses the possible application; and finally the conclusions are summarized in section 6.

2 Description of experiment setup

2.1 Measurement location

The Integrated Microwave Radiometry Campaign for snow (IMCS) was performed during snow season of 2015/2016 (from November 27, 2015 to March 25, 2016) at the Altay National Reference Meteorological station (ANRMS) (N47º44'26.58", E 88º4'21.55") which is at the foot of Altay mountain in the northwest China, and approximate 6 km distance from the mountain (Figure 1). Altay mountain, running northwest and southeast, is at the junction of China, Russia, Mongolia and Kazakhstan, and the elevation is up to 3000 m, providing snow water resources for the four countries. The average annual maximum snow depth measured in this station is approximately 40 cm, and the maximum value is over 70 cm. In the southwest of Altay mountain, crop land and desert with flat terrain are the dominant land covers. Snow cover is critical fresh water for the irrigation in this area. In this experiment, measurements included microwave radiometry, 4-component radiation, snow pit and soil parameters. The test site of this experiment was four neighboring bare rectangle fields in the ANRMS with their area of 2500m^2 (black rectangle filed in Figure 1), 2500m^2 (pink rectangle field in Figure 1), 200m^2 (red rectangle field in Figure 1) and 400 m^2 (blue rectangle field in Figure 1), respectively.

In the pink field, the ground-based microwave radiometer was set up in the middle place of this field, facing south to collect brightness temperatures of snow cover. The black field behind the microwave radiometers (north of the radiometers) was for snow pit data collection. The microwave

https://doi.org/10.5194/essd-2022-68
Preprint. Discussion started: 4 March 2022

radiometer observations and snow pit data collection were conducted by Northwest Institute of Eco-Environment and Resources, Chinese Academy of Science (NIEER) from November 27, 2015 to March 25, 2016 (After March 25, 2016, snow melted out).

The blue field is for meteorological measurements including wind speed, wind direction, air temperature, air wetness, air pressure, precipitation, layering soil temperature, soil moisture among others. These parameters were automatically obtained from instruments, and the instruments setup and data collection were operated by ANRMS. This station also has daily manual observation in snow depth and SWE. In this experiment, we requested the wind, air pressure, air wetness, soil temperature and moisture data during this experiment from ANRMS.

The red field was designed for automatic measurement of layering snow temperatures, snow density, SWE, snow depth, and albedo. These automatic measurement instruments were installed and maintained by NIEER, and started working from 2013. However, during the experiment, the instruments for snow density and SWE did not work, and we only collected layering snow temperatures and 4-component radiation from November 27, 2015 to March 25, 2016.

Because the four observation fields are located within the domain of the station and the distance between each other are less than 100m, the snow characteristics and soil and weather conditions are thought to be the same. Ultimately, the collected data in this study include ground-based brightness temperatures, 4-component radiation, snow pit data, meteorological data and automatically observed layering snow and soil temperatures.

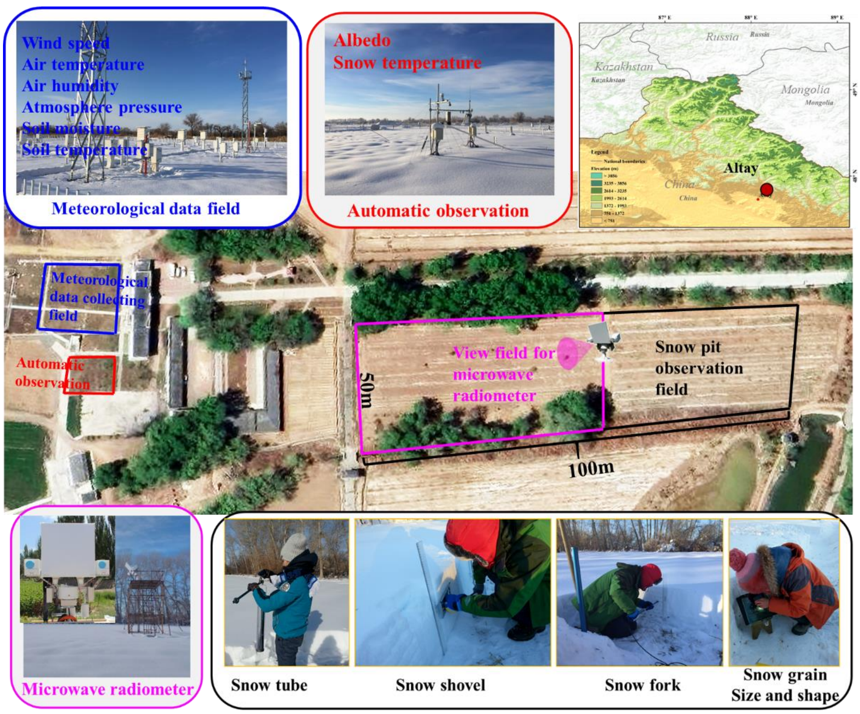

Figure 1: Location of the Altay National Reference Meteorological station (ANRMS) in the Asia and the distribution of three experiment fields in the ANRMS. The black rectangle represents the field used for snow characteristics (approximately 40 m × 50 m) including layering thickness, snow density, snow grain size and

https://doi.org/10.5194/essd-2022-68
Preprint. Discussion started: 4 March 2022

shape, and microwave radiometers (approximately 60 m × 50 m) observations. The blue rectangle is the field for Meteorological and soil data collection operated by the ANRMS. The red rectangle field is for the automatically observation of the snow temperature, SWE, 4-component radiation and snow depth, designed by Northwest Institute of Eco-Environment and Resources, Chinese Academy of Science (NIEER). Note: The map in the up right corner is ArcGIS self-contained map.

2.2 Measurement parameters and instruments

The brightness temperatures at 1.4, 18.6, 36.5 GHz for both polarization (Tb1h, Tb1v, Tb18h, Tb18v, Tb36h, Tb36v) were automatically collected using a six-channel dual polarized microwave radiometer RPG-6CH-DP (Radiometer Physics GmbH, Germany, https://www.radiometerphysics.de/products/microwave-remote-sensing-instruments/radiometers/). The technical specifications of the RPG-6CH-DP are described in Table 1. The RPG-6CH-DP contains a built-in temperature sensor which can measure air temperature. The automatically data collection frequency was set as 1 minute.

Table 1. Technical Specifications of the RPG-6CH -DP Microwave Radiometer.

Parameter	Value
Manufacturer	Radiometer Physics GmbH
System noise temperatures	<900 K
Bandwidth	400MHz (20MHz for 1.4 GHz)
System stability	0.5 K
Dynamic range	0~400 K
Frequencies (GHz)	1.4, 18.7, 36.5
Polarizations	V, H
Internal calibration	Internal Dicke switch and software control for automatic sky tilt calibration
Receiver and antenna thermal stabilization	< 0.015 K
Antenna sidelobe level	< -30 dBc
Optical resolution (HPBW)	6.1° (11° for 1.4 GHz)
Incidence angle	0~90°
Azimuth angle	360°

The microwave signatures from snowpack vary with snow characteristics, soil and weather conditions. The snow characteristics were obtained by manual snow pit measurements in the black field, including layering snow thickness, layering grain size, snow density, and snow temperatures. These data were daily collected during 8:00-10:00 am local time, from November 27, 2015 to March 25, 2016, except 7 days (please see Table 1). Although the snow temperatures were manually measured at snow pits, the automatically collected snow temperatures in the red field were utilized in this study, because the temperature measured at snow pits could not reflect the natural temperature profile when the snow pits exposed to the air. In the red field, the 4-component radiation was automatically measured by NR01 manufactured by Hukseflux, and layering snow temperatures was measured by Campbell 109S temperature sensors, respectively. The soil and weather parameters are of routine observations at

https://doi.org/10.5194/essd-2022-68
Preprint. Discussion started: 4 March 2022

Open Access Earth System Science Data Discussions

ANRMS, and were obtained through request from ANRMS. The instruments used for soil and weather parameters observations are produced by China Huayun Meteorological Technology Group corporation. The measurement parameters and their measurement instruments are listed in table 2.

Table 2. Variables collected in MRESC and the observation equipment, observation time and frequencies.

Parameter	Equipment/Method	Layering style	Observation time or frequency	Absent date
Tb1h, Tb1v, Tb18h, Tb18v, Tb36h, Tb36v and air temperature	Microwave radiometers RPG-6CH-DP/ Automatically	5 meters above ground	minutely	no
Layer thickness (cm)	Ruler / Manually	Natural layering	local time 8:00-10:00 am	no
Snow density (g/cm3)	Snow tube / Manually	Whole snowpack	local time 8:00-10:01 am	no
Snow density (g/cm3)	Snow shovel/ Manually	Every 10 cm	local time 8:00-10:02 am	1/2-3/2016, 2/20/2016
Snow density (g/cm3) and liquid water content (%)	Snow fork/ Manually	At interval of 5 cm from the 5-cm height	local time 8:00-10:03 am	
Snow grain size (mm)	Anyty V500IR/UV/ Manually	Natural layering	local time 8:00-10:04 am	12/24/2015, 12/31/2015, 1/1-3/2016, 1/23/2016, 2/20/2016
Snow grain shape	Visually identification/ Manually	Natural layering	local time 8:00-10:05 am	
Snow temperature(°C)	Temperature sensors (Campbell 109S) / Automatically	0 cm, 5 cm, 10 cm, 15 cm, 25 cm, 35 cm, 45 cm, and 55 cm	Ten-minute	no
4-component radiation (W/m2)	Component Net Radiometer (NR01) / Automatically	6 feets above ground	Ten-minute	no
Soil temperature(°C)	Soil temperature sensor (China Huayun) / Automatically	5cm below soil/snow surface (-5cm)	Hourly	no
Soil moisture (%)	Soil moisture sensor (DZN3, China Huayun) / Automatically	10cm below soil/snow surface (-10cm)	Hourly	no
Air temperature(°C)	Thermometer screen (China Huayun) / Automatically	6 feets above ground	Hourly	no

https://doi.org/10.5194/essd-2022-68
Preprint. Discussion started: 4 March 2022

Air pressure (Pa)	Thermometer screen (China Huayun) / Automatically	6 feets above ground	Hourly	no
Air humidity (%)	Thermometer screen(China Huayun) / Automatically	6 feets above ground	Hourly	no
Wind speed (m/s) and direction	Wind sensor(China Huayun) / Automatically	10 m above ground	Hourly	no

2.3 Measurement methods

In this experiment, the measurements include microwave radiometry observation to collect brightness temperature, snow pit observation to collect snow physical parameters, automatic observation to collect 4-component radiation and snow temperatures, and meteorological observation which contains weather data and soil data.

2.3.1. Microwave radiometry

Before snow season, a platform with height of 5 m, length of 4 m and width of 2 m was constructed in the experiment field. A 4-m orbit was fixed on the platform. The RPG-6CH-DP was set up on the orbit and could be moved along the orbit. This radiometer was sky tipping calibrated. In the clear sky conditions, the sky brightness temperatures are approximately 7.8$\pm$1K and 15.7$\pm$0.7K at 1.4 GHz for horizontal polarization and vertical polarization, respectively; those were approximately 29.7$\pm$0.3 K and 29.3$\pm$0.9 K at 18.7GHz and 36.5 GHz, respectively.

Generally, the radiometers were fixed in the middle place of the orbit to observe snow cover with incidence angle of 45°. Multi-angle observations were conducted on seventeen days (Dec 3, Dec 19, Dec 30, Jan 3, Jan 8, Jan 13, Jan 18, Jan 23, Jan 28, Feb 3, Mar 3, Mar 10, Mar 15, Mar 22, Mar 26, Mar 28, Mar 31) when the radiometer was set to scan the ground at different incidence angles at two ends of the orbit and the middle place of the orbit. Although the view fields of the antennas for 1.4 GHz, 18 GHz and 36 GHz did not completely overlap, the measured results showed that the brightness temperatures observed by radiometers at the left, middle and right of the orbit varied less than 1 K. Therefore, the snow and soil characteristics presented homogeneous distribution within the view files of the three antennas.

2.3.2 Snow pit measurement

The physical snow parameters were measured at snow pits. These parameters included snow depth, snow density, snow layering, layering grain size and shape type, layering snow density.

The first step of snow pit measurement is making snow pit. In the black field, snow pits were made every day. A spade was used to excavate snow pit. The length of the snow pit profile was approximately 2m to make sure all parameters were measured from unbroken snowpack. The width of the snow pit was approximately 1m for observers to conveniently observe. The snow pit section was made as flat as possible using a flat shovel or ruler. When the snow profile expose to the air for a long time, the snow characteristics will be influenced by environment and will be different from the natural snow characteristics. In order to make sure every observation conducted on natural snow pit, the snow pit was

https://doi.org/10.5194/essd-2022-68
Preprint. Discussion started: 4 March 2022

Open Access Earth System Science Data Discussions

backfilled with the shoveled snow after finishing all observations, and the new snow pit in the following day was made at least 1-m distance from the last snow pit.

The second step of snow pit measurement was recording the natural stratification. After finishing a snow pit, the natural stratification of snowpack was firstly visually determined against a ruler, and the snow thickness of every layer was recorded.

The third step was measuring grain size and shape type in each layer, whilst snow density was measured at constant interval. The grain size and type within each natural layer were estimated visually from a microscope with a camera named "Anyty V500IR/UV" (Figure 2a). A software matched the microscope was used to measure the grain size. The grain type was determined based on Fierz et al. (2009). In this experiment, we utilized the length of longest axes and the length of shortest axes to describe grain size (Figure 2b). When using the software to measure the grain size, a reference must be needed. In this experiment, the minimum scale "0.5mm" of a ruler was used as reference (Figure 2c). We adjusted the focus of the camera to make sure the grains at the clearest status in camera to take photos, and the photo of ruler scale was taken at the same focus. If the thickness of one layer was less than 10 cm, measurements were performed at the top and bottom of the layer. If the thickness was greater than 10 cm, measurements were performed at the top, middle, and bottom of the layer. For each layer, at least 5 photos were taken, and at least 10 typical grains were chosen to measure the longest axes length and the shortest axes length in the photos of each layer. Then, in each layer, there were at least 10 groups of the longest and shortest axes length were obtained, and the final grain size was the average values. Figure A1 presents an example of the original photos of grains in each layer, and Table A1 shows the matched record of longest and shortest axis length.

(a) (b) (c)

Figure 2: Picture of microscope "Anyty V500IR/UV" (a), the measured longest axes lengths and shorteast axes length of particles (b), and the reference ruler scale (c).

Snow density was measured using three instruments: snow tube, snow shovel and Snow Fork (Figure 3). The snow tube instrument, designed by Chinese Meteorological administration, contains a metal tube with the base area of 100 cm^2 and the length of 60 cm, and a balance (figure 3a). It was utilized to measure the snow density of a whole snowpack by weighing the snow sample. The snow shovel is a 1500 cm^3 wedge-type sampler, and its length, width and height are 20 cm, 15 cm, and 10 cm, respectively (figure 3b). It was utilized to measure layering snow density every 10 cm (0-10 cm, 10-20 cm, 20-30 cm…). The Snow Fork is a microwave resonator that measures the complex dielectric constant of snow, and adopts a semi-empirical equation to estimate snow density and liquid water content based on the complex dielectric. The Snow Fork (figure 3c) was utilized to measure snow density and liquid water content at 5-cm intervals from the 5-cm height over the snow/soil interface (5cm, 10cm, 15 cm, 20cm…). Table A2 is an example of record table for snow density. Three times of observations were conducted for

https://doi.org/10.5194/essd-2022-68
Preprint. Discussion started: 4 March 2022

every layer.

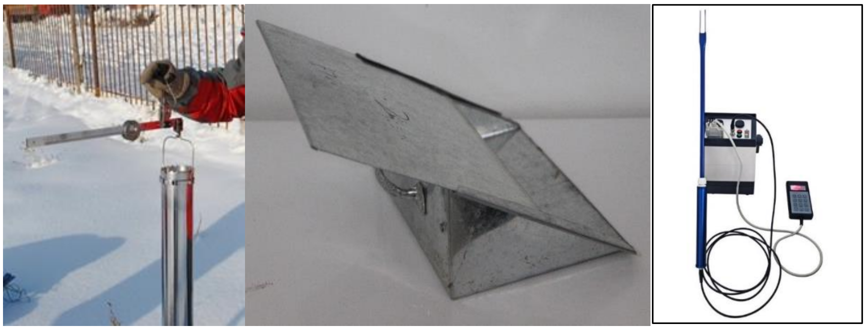

(a) (b) (c)

Figure 3: Three instruments for snow density: Snow tube (a), Snow shovel (b), and Snow Fork (c).

2.3.2 Automatic radiation and temperature measurement

Layering snow temperatures were collected using Temperature sensors at the red field instead of manual observation from snow pits. The temperature sensors had been set up on a vertical pole which was vertically inserted in the soil (Figure 4). The heights of the sensors are 0 cm, 5 cm, 10 cm, 15 cm, 25 cm, 35 cm, 45 cm, and 55 cm. The snow temperatures at these heights were collected every minute.

TheNR01 net radiometer was set up to measure the energy balance between incoming short-wave and long-wave Far Infrared radiation versus surface-reflected short-wave and outgoing long-wave radiation. The range of short wave is 285~3000nm, and the range of long wave is 4.5~40um. The 4-component radiation was automatically recorded every ten minutes. In addition, the sensor is equipped with a Pt100 temperature sensor for parallel recording of the sensor temperature.

https://doi.org/10.5194/essd-2022-68
Preprint. Discussion started: 4 March 2022

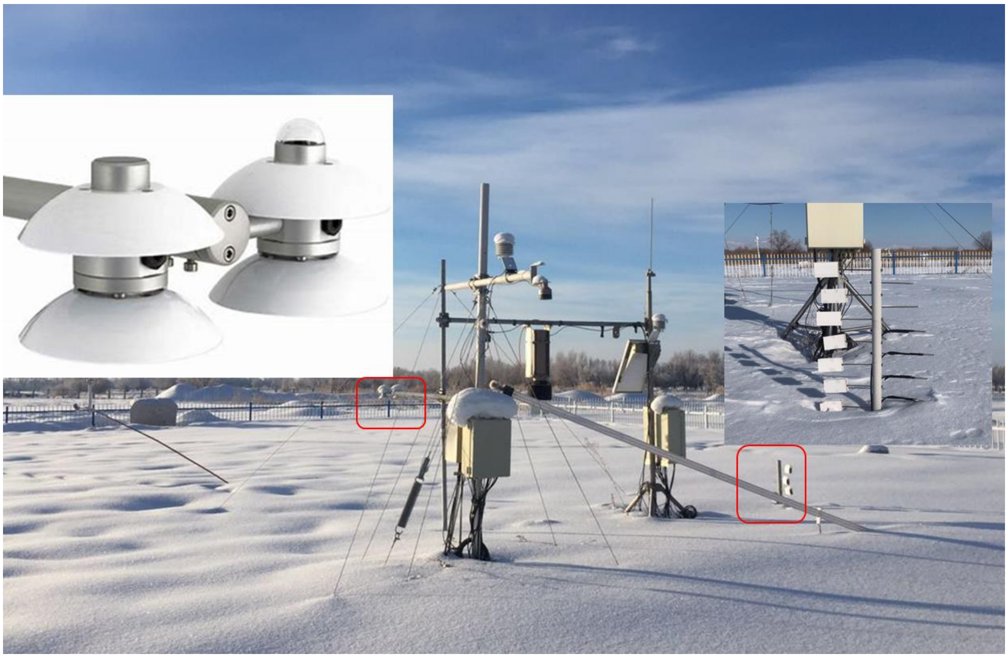

Figure 4: Set up of temperature sensors and CNR4 in the red field.

2.3.3 Meteorological observation

The meteorological data requested from the ANRMS include air temperature, air pressure and humidity, wind speed, soil temperature at -5cm, -10 cm, -15cm and -20 cm and soil moisture at -10 cm and -20 cm.

The air temperature, pressure and humidity were collected using temperature and wetness sensor in thermometer screen, the wind speed and direction were measured using wind sensor set up at 10 m on a tower. Soil moisture and temperature were automatically measured using moisture sensor and temperature sensor. Figure 5 depicts the instruments for these observations.

(a) (b) (c) (d)

Figure 5: Instruments for observation of air temperature and wetness (a), wind speed (b), soil temperature (c) and soil moisture (d).

https://doi.org/10.5194/essd-2022-68
Preprint. Discussion started: 4 March 2022

3 Description of consolidated IMCS data

The microwave brightness temperature, snow parameters, meteorological data were recorded in different formats, and the observation frequencies and times were different. These data must be reorganized or consolidated for easily usage. The values from the three-time measurements for snow density in each layer were averaged to obtain the final snow density. The length of the longest and shortest axes of particles in each photo were measured using the software. The average lengths of longest and shortest axes from all photos in each layer were obtained as the final grain size.

The ground-based brightness temperatures and layering snow temperatures were automatically collected in uniform format. The weather and soil data requested from ANRMS had been consolidated. Finally, the provided datasets are as following and table 3 describes the contents of each dataset.

1) Brightness temperatures data:

1 Minutely calibrated brightness temperature at 1.4 GHz, 18 GHz and 36 GHz for both polarizations at incidence angle of 45°. This data include date, time, brightness temperatures at the three bands for both polarizations.

2 Seventeen groups of calibrated brightness temperature at 1.4 GHz, 18 GHz and 36 GHz for both polarizations at different incidence angles (30, 35, 40, 45, 50, 55, 60°). This data include date, incidence angles, brightness temperatures at the three bands for both polarizations.

2) Snow pit data:

1 Daily grain size data include date, snow depth, layering snow thickness, average longest axis, average shortest axis of each layer. The data were stored in an excel sheet.

2 Daily snow density data include date, layering snow density using snow fork (snow density at different heights, such as SF_5cm, SF_10cm, SF_15cm), snow density using snow tube, layering snow density using snow shovel (such as SS_0-10cm, SS _10-20cm, SS _20-30cm, SS _30-40cm). The data were stored in an excel sheet.

3 Ten-minute snow temperatures data include date, time, temperatures at different heights (such as ST_0cm, ST_5cm).

3) Snow surface radiation data

1 4-component radiation data include date, time, short-wave incident radiation, short-wave reflected radiation, long-wave infrared incident radiation, long-wave infrared reflected radiation, and sensor temperature.

4) Meteorological data:

1 Hourly weather data include date, hour, air temperature, wetness and humidity wind speed and direction.

2 Hourly Soil data include date, hour, soil temperature at 5 cm, 10 cm, 15 cm and 20 cm, and soil moisture at 10 cm and 20 cm.

These data were stored in four folders, and different parameters were stored in different excel table or ascii files. The organization of these consolidated data were described in table 3.

Table 3 Description of consolidated data

Folder	Data	Store format	Content
Brightness temperature	Minutely brightness temperature	Ascii file	Date, time, Tb1h, Tb1v, Tb18h, Tb18v, Tb36h, Tb36v

https://doi.org/10.5194/essd-2022-68
Preprint. Discussion started: 4 March 2022

	Multi-angle brightness temperatures	Ascii file	Date, time, incidence angle, Tb1h, Tb1v, Tb18h, Tb18v, Tb36h, Tb36v
	Grain size	Excel sheet	Date, snow depth, th1, Lg1, Sg1, th2, Lg2, Sg2,th3, Lg3, Sg3, th4, Lg4, Sg4,th5, Lg5, Sg5, th6, Lg6, Sg6
Snow pit data	Snow density	Excel sheet	Date, Stube, SS_0-10, SS_10-20, SS_20-30, SS_30-40, SS_40-50, SF_5, SF_10, SF_15, SF_20, SF_25,SF_30,SF_35,SF_40,SF_45,SF_50,
	Snow temperature	Excel sheet	Date, time, snow depth, ST_0cm, ST_5cm, ST_15cm, ST_25cm, ST_35cm, ST_45cm, ST_55cm
Radiation data	4-component radiation	Excel sheet	Date, time, SR_DOWN, SR_UP, LR_DOWN, LR_UP, T_Sensor
Meteorological data	Hourly weather data	Excel sheet	Date, hour, Tair, Wair, Pair, Win
	Hourly soil moisture and temperature	Excel sheet	Date, SM_10cm, SM_20cm, Tsoil_5cm, Tsoil_10cm, Tsoil_15 cm, Tsoil_20cm

Note: th: snow thickness, Lg: long axis, Sg: short axis;
Stube: snow density observed using snow tube, SS: snow density observed using snow shovel, SF: snow density observed using snow fork; ST: snow temperature; SR_DOWN: downward short-wave radiation, SR_UP: upward short-wave radiation, LR_DOWN, downward long-wave radiation, LR_UP: upward long-wave radiation, T_sensor: sensor temperature; Tair: air temperature, Wair: air wetness, Pair: air pressure, Win: wind speed.

4 Overview of collected data from IMCS

4.1 Snow characteristics

4.1.1 Layering grain size and grain shape

During winter of 2015/2016, snow cover began on 25 November of 2015, and ended on March 25 of 2016. During this snow cover duration, seven snowfall events occurred, and each snowfall formed one layer in snow cover on the ground, except the third event which presented a new layer on the second layer at the beginning, but the layering interface disappeared after several days and visually displayed as one layer (in gray in Figure 6). The fourth event was biggest of all, and the depth of snow cover exhibited decreasing with increase of snow density after the fourth event. Snow cover began melting on March 14 and snow depth declined to zero within 10 days.

Grain sizes within all layers exhibited increasing during the snow season, except in the bottom layer where grain size experienced a decrease from December 28 to January 20 (Figure 7). In the vertical profile, grain size increased from up to down with the snow age. The grain size of the fresh snow was approximately 0.3 mm. The biggest long and short axis were up to 6 cm and 4 cm, respectively, which occurred within Layer 1 in the melting period. The length of short axes is approximately 0.7 of the length of long axes. The grain shape generally developed from rounded grains to facet crystals, and then to depth hoar. After March 13, 2016, the minimum air temperature increased to above 0, snowpacke accelerately melted, and the grain shape developed to melted forms.

https://doi.org/10.5194/essd-2022-68
Preprint. Discussion started: 4 March 2022

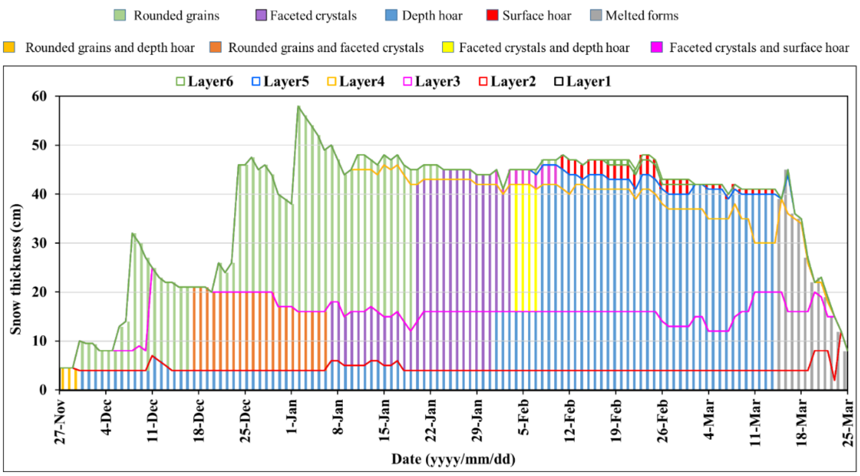

Figure 6: Daily variation in layering grain shape from November 27, 2015 to March 25, 2016.

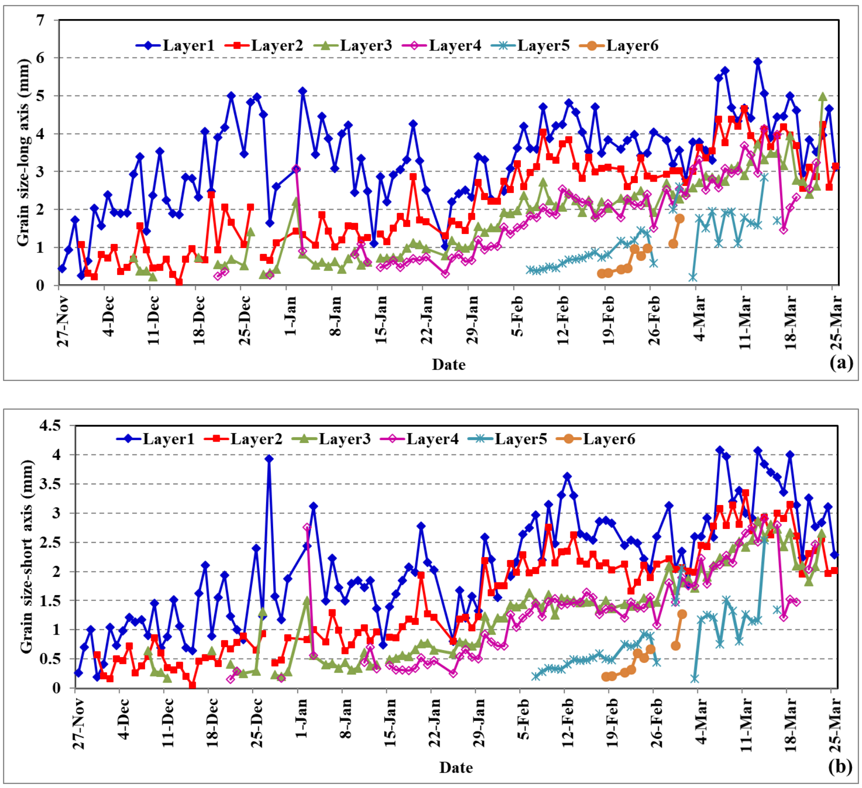

Figure 7: Daily variation in grain size within each layer from November 27, 2015 to March 25, 2016. The thickness of each layer is presented in figure 9.

4.1.2 Snow density

Snow densities measured by three different equipment shows that the density of fresh snow ranged

https://doi.org/10.5194/essd-2022-68
Preprint. Discussion started: 4 March 2022

between 0.05~1.0 g/cm3 (Figure 8). The snow densities increased with snow age, and kept stable when the value arrived at 0.2~0.25g/cm3. From March 14 on, snow densities abruptly increased. The biggest value was beyond 0.45g/cm3. In the vertical profile, snow density increased from up to down in the accumulation phase, but in the stable phase, snow densities in the middle layers were larger than those in the bottom and upper layers. In the melting phase, snow densities in all layers showed little difference.

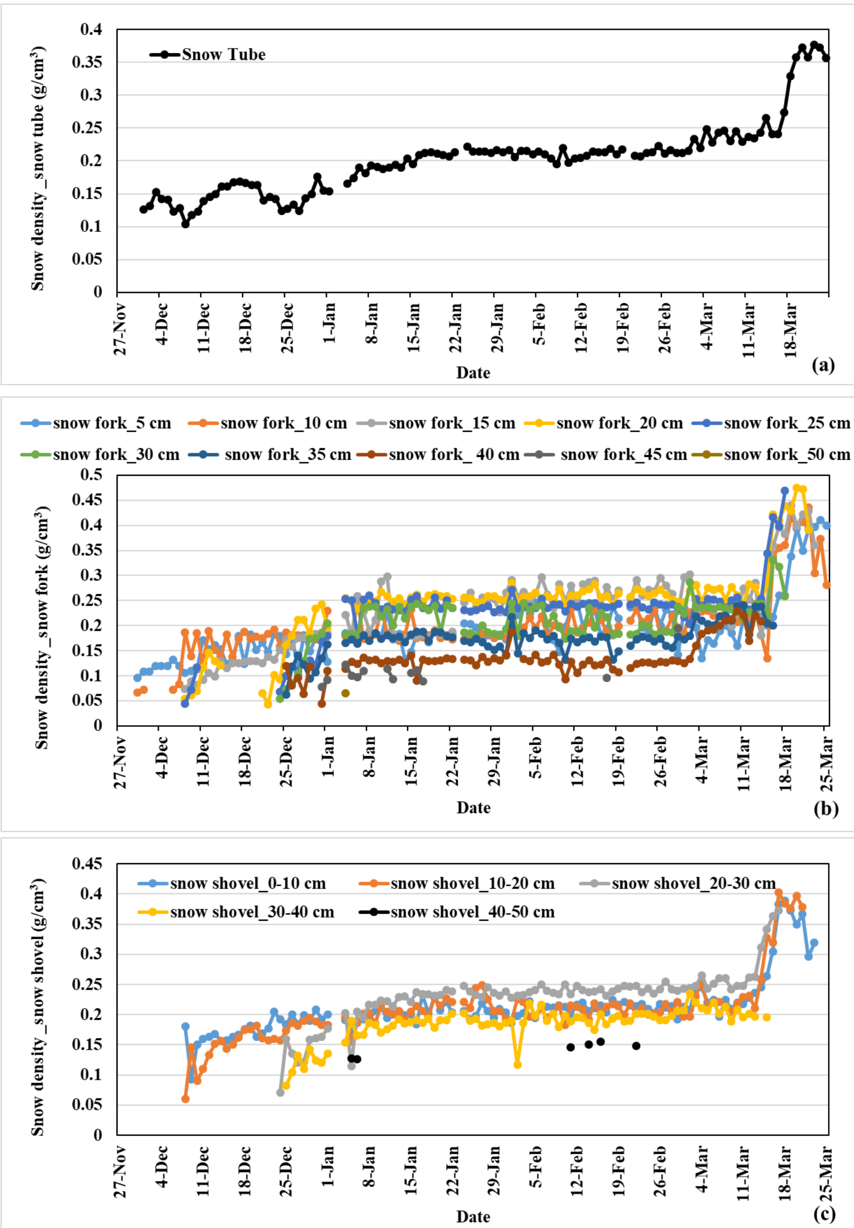

Figure 8: Daily variation in snow densities measured using three different measurement methods from November 27, 2015 to March 25, 2016.

https://doi.org/10.5194/essd-2022-68
Preprint. Discussion started: 4 March 2022

4.1.3 Snow temperature

Snow temperature at 0 cm (snow/soil interface temperature) showed little diurnal variation, remaining at approximately -2.0 to 0.7°C. Snow temperature at top layer exhibited largest diurnal variation. The diurnal variation range decreased from top to bottom layers, and with the increase of snow depth, temperatures in more layers presented small diurnal variations (Figure 9). After March 17, 2016, the snow temperature of all layers were over 0°C which means snow cover did not refreeze anymore.

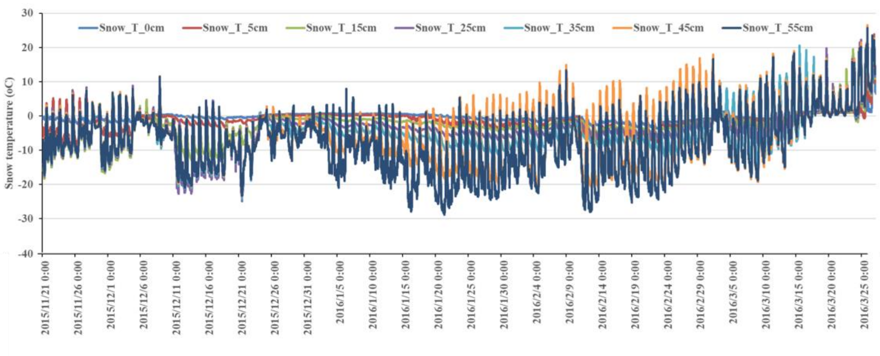

Figure 9: Variation in layering snow temperatures during experiment time.

4.2 Soil temperature and moisture

The soil temperature at 5 and 10 cm remained below 0 ºC and stable during the snow season, but presented large fluctuation before snow cover onset and after snow off (Figure 10). The temperature gaps between 5 cm and 10 cm were much larger before snow cover onset than those during snow cover duration. The soil moistures at 10 cm were above 10% before snow cover onset and after snow off, and were below 10% during the snow cover duration. During Dec 12-14, and Jan 1- 20, soil moisture showed peak value, which corresponded to the two high-value periods of soil temperature.

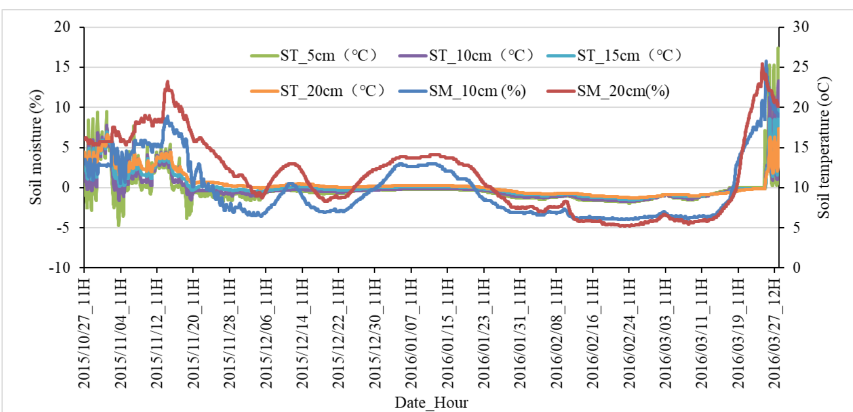

Figure 10: Hourly variation in soil temperature at 5 cm,10 cm, 15cm and 20 cm, and soil moisture at 10cm and 20cm.

https://doi.org/10.5194/essd-2022-68
Preprint. Discussion started: 4 March 2022

4.3 Brightness temperature

The microwave brightness temperatures varied with snow and soil characteristics, and weather conditions. Figure 11a shows the daily brightness temperatures, brightness temperature difference between 18 and 36 GHz, snow depth and air temperature at 1:00 am, and Figure 11b shows the hourly variation in brightness temperatures at the three frequencies and air temperature after February 1. Data depict that Tb36h and Tb36v decreased during the whole snow season, Tb18h show obvious decline after Feb 18, and Tb18v show decline after Mar 3 for vertical polarization (Figure 11a). After Jan 4, snow depth stopped increasing, but the brightness temperature continued to decrease and brightness temperature difference increased. Based on Figure 8, snow density arrived at stable on Jan 15. Therefore, after Jan 4, the decreasing brightness temperatures was mainly caused by growing grain size.

After Feb 25, brightness temperature exhibited abrupt increase (at day time) - decrease (at night time) circle (Figure 11b), because air temperature at noon increasing up to above 270 K resulted in large liquid water content at day time, and the melted snowpack refroze when air temperature decreased at night time and brightness temperature decreased. After March 14, air temperature presented another big rise and even the night air temperatures were above 270 K; snow cover accelerated melting, and the liquid water could not be completely refrozen; then brightness temperature and brightness temperature difference exhibited unregularly variations.

The variation of L band was mainly influenced by soil moisture and soil temperature. We have soil temperatures at 0cm, 5 cm and 10 cm and soil moisture at 10 cm. However, the L band reflects the soil moisture within 5 cm which was absent in this experiment. Actually, we did not find the variation of brightness temperature at L band had relationship with soil moisture at 10 cm and soil temperature.

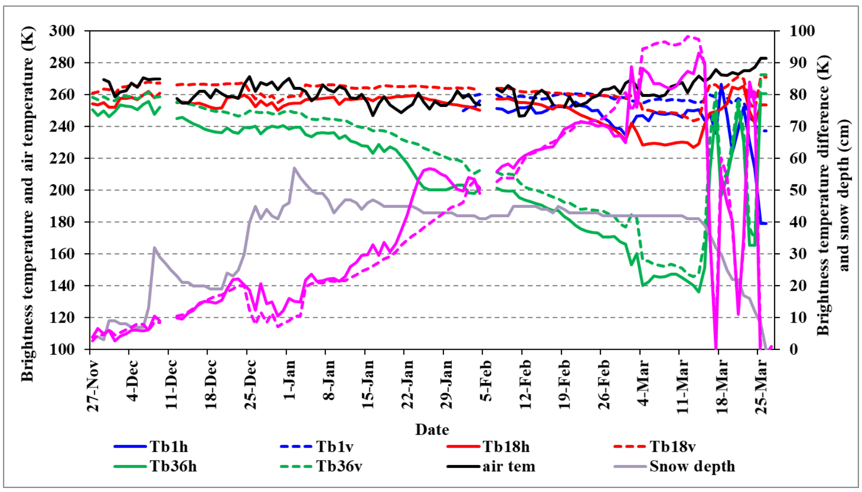

.

https://doi.org/10.5194/essd-2022-68
Preprint. Discussion started: 4 March 2022

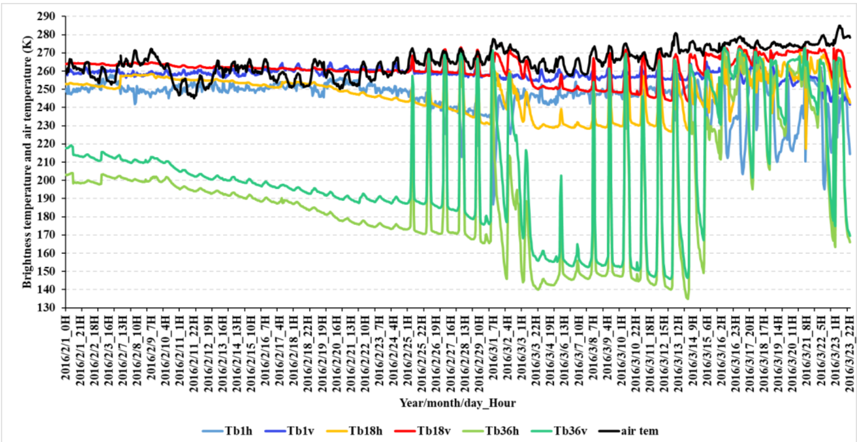

Figure 11: (a) Daily variations in brightness temperatures at 1.4 GHz, 18 GHz and 36 GHz, for horizontal (Tb1h, Tb18h, Tb36h) and vertical polarizations (Tb1v, Tb18v, Tb36v), and the differences between Tb18h and Tb36h (TBDh), and between Tb18v and Tb36v (TBDv), at 1:00 am (local time), from November 27, 2015 to March 26, 2016. (b) hourly variation in Tb1h, Tb18h, Tb36h, Tb1v, Tb18v, Tb36v, from February 1 to March 23, 2016.

The brightness temperatures from AMSR-2 were compared with the ground-based observation at the overpass time (Figure 12). Although there was large difference between them, the general variations are the same, even for the abrupt change between Mar 3 and Mar 4, and the correlation coefficients at both polarizations were approximately 0.96 and 0.7 for 36 GHz and 18.7GHz, respectively. Satellite observed brightness temperature presented less decrease trend than ground-based observation, and the difference at 36 GHz is larger than at 18 GHz (Figure 12). The difference between ground-based and satellite observation might be attributed to the different viewing area.

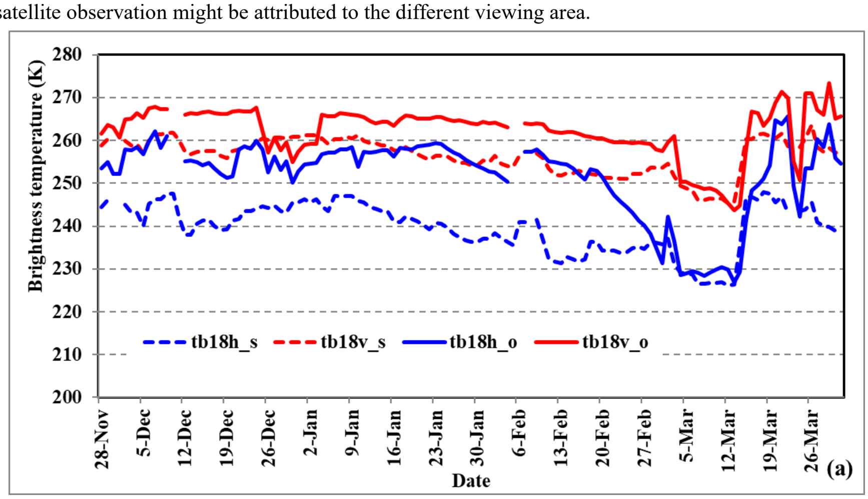

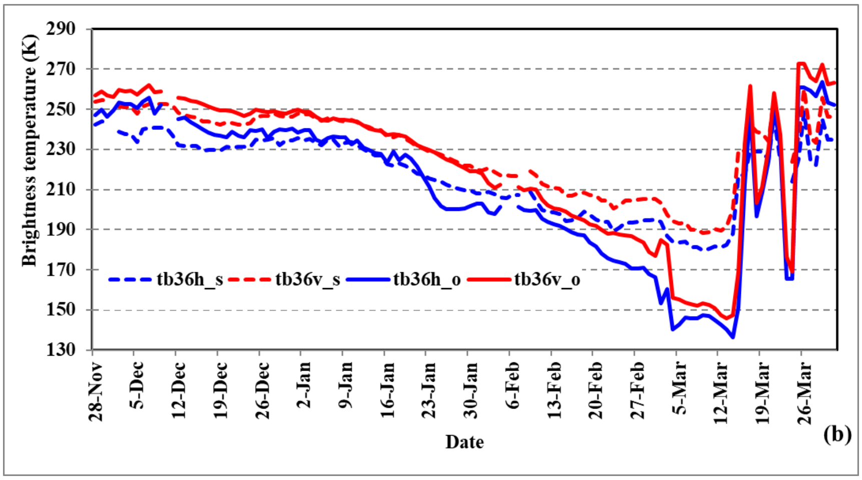

Figure 12: Comparison of brightness temperature between ground-based and Satellite-based observation (s: satellite; o: observation), (a) for 18 GHz, (b) for 36 GHz.

4.4 4-component Radiation

The land surface albedo is strongly related to the land cover. In this experiment, the down-short wave radiation presented general increase after January, and the trend became distinctive after February (Figure 13). The upward short-wave radiation abruptly increased when the ground was covered by snow, and sharply declined on the snow off day. From the first snowfall to the end of January, the ratios between upward and downward short-wave radiation were approximately 95%. The ratio decreased with snow age, and in the end of snow season the ratios decreased to below 50% because of increasing melted water.

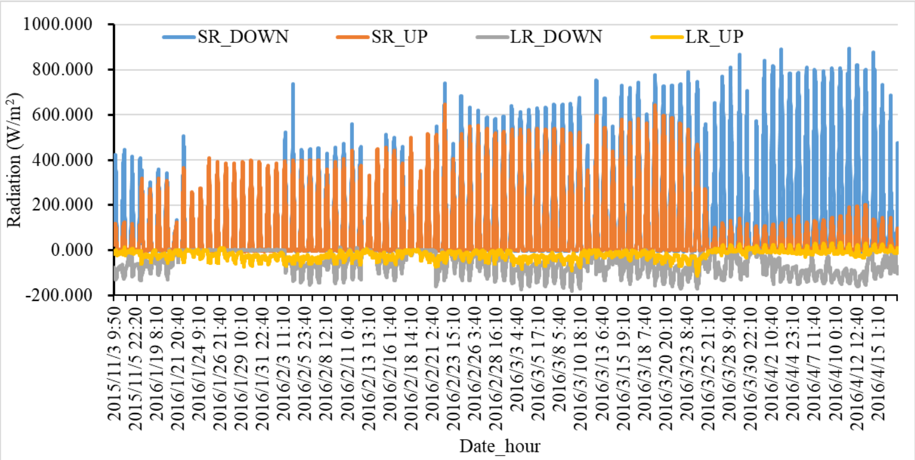

Figure 13: Minutely variation in 4-component radiation at Altay station from November 3 2015 to April 15 2016.

https://doi.org/10.5194/essd-2022-68
Preprint. Discussion started: 4 March 2022

5 Discussion

This experiment provided a suite of snow characteristics and microwave brightness temperatures, and have proven useful for evaluating and updating microwave emission transfer model of snowpack (Dai et al., 2021). This dataset reflected the general fact that brightness temperature at higher frequencies presented stronger volume scattering of snow grains, and were more sensitive to snow characteristics. This experiment revealed that the dominant control factor for the variation of brightness temperature was the variation of grain size but not the snow depth. The largest snow depth or SWE does not correspond to the largest brightness temperature gradient in the condition of dry snowpack. Due to the growth of grain size, the peak gradient occurred before melting for stable snow cover. Therefore, the daily snow depth variations curve derived from passive microwave remote sensing datasets tend to exhibit a temporal offset from those of in situ observation.

During the snow season, brightness temperatures for both polarizations presented similar variation, but they behaved different in some temporal periods. The horizontal polarization was more sensitive to environment and demonstrated less stable than vertical polarization. Besides, the polarization difference at 18 GHz and 36 GHz showed increase and decrease trends, respectively during the experimental period. The results for 18 GHz were opposite to the simulation results (Dai et al., 2021). These phenomena must rely on the environmental conditions, snow characteristics and soil conditions. However, the subsurface soil wetness data were absent, the dynamic ground emissivity could not be estimated. L band has strong penetrability, and the brightness temperature variations were dominantly related to subsurface soil condition, except when the liquid water content within snowpack was high. Therefore, although we did not have soil moisture data in the subsurface layer, L band brightness temperatures were expected to retrieve soil moisture variation which influence the soil transmissivity (Babaeian et al., 2019; Naderpour et al., 2017; Hirahara et al., 2020).

Snow surface albedo significantly influence the incoming solar radiation, playing an important role in climate system. The factors to change the snow surface albedo essentially contains the snow characteristics (grain size, SWE, liquid water content, impurities, surface temperature etc), external atmospheric condition and solar zenith angle (Aoki et al., 2003). Snow albedo was estimated based on snow surface temperatures in some models (Roesch et al., 1999), and some models considered snow surface albedo mainly depends on snow aging (Mabuchi et al., 1997). In this experiment, we obtained the 4-component radiation, snow pit and meteorological data. These data provide nearly all observations of possible influence factors, and could be utilized to discuss and analyze shortwave radiation process of snowpack, and validate or improve multiple-snow-layer albedo model.

Snow grain sizes and snow densities within different layers presented different growth rates at different temporal phase. Generally, the growth rates are related to the air temperature, pressure and snow depth (Chen et al., 2020; Essery, 2015; Vionnet et al., 2012; Lehning et al., 2002); therefore, this dataset can be used to analyze the evolution process of snow characteristics, as well as validation data for snow models.

6 Conclusions

In a summary, the IMCS campaign provides a time series of snow pits observation, meteorological parameters, optical radiation and passive microwave brightness temperatures in the whole snow season of 2015/2016. The dataset is unique in providing microwave brightness temperatures and matched daily snow pits data over a snow season at the fix site.

The dataset contains the unique daily snow pit data which present detail description of snow grain size, snow density and snow temperature profiles. It can be used to analyzes the evolution process of snow characteristics, validating or improving the snow process models, such as SNOWPACK (Lehning et al., 2002), SNTHERM (Chen et al., 2020). The improvement of these models can further enhance the prediction accuracy of land surface process and hydrology models, and the simulation accuracy of snow microwave emission models.

Actually, this dataset has been utilized to analyze the volume scattering features of snow pack at different frequencies (Dai et al., 2021). It can also be used to further analyze polarization characteristics of snow pack, and be used to validate different microwave emission models of snowpack.

Moreover, in this experiment, the microwave and optical radiations were simultaneously observed. The existing studies reported that the optical equivalent diameter must be used in microwave emission model with caution (Lowe and Picard, 2015; Roy et al., 2013). It is a good chance to analyze the difference between the influence of grain size on microwave and optical radiation, establishing the bridge between effective optical grain size and microwave grain size.

7 Data availability

The IMCS consolidated datasets are available after registration on the National Tibetan Plateau Data Center and available online at https://data.tpdc.ac.cn/en/ (doi: 10.11888/Snow.tpdc.270886). Microwave radiometry raw Data are available for scientific use on request from Northwest Institute of Eco-Environment and Resources, Chinese Academy of Sciences.

Author contributions: LD and TC designed the experiment. LD, YZ, JT, MA, LX, SZ, YY YH and LX collected the passive microwave and snow pit data. HL provided the 4-component radiation and snow temperature data. LW provided meteorological data. LD write the manuscript, and TC made revision. All authors contributed to the data consolidation.

Competing interests: The authors declare that they have no conflict of interest.

Acknowledgment: The authors would like to thank the Altay meteorological station for providing logistics service and meteorological data.

Financial support: This research was funded by the National Science Fund for Distinguished Young Scholars (grant nos: 42125604), National Natural Science Foundation of China (grant nos: 42171143), and CAS 'Light of West China' Program.

https://doi.org/10.5194/essd-2022-68
Preprint. Discussion started: 4 March 2022

Open Access Earth System Science Data Discussions

Appendix

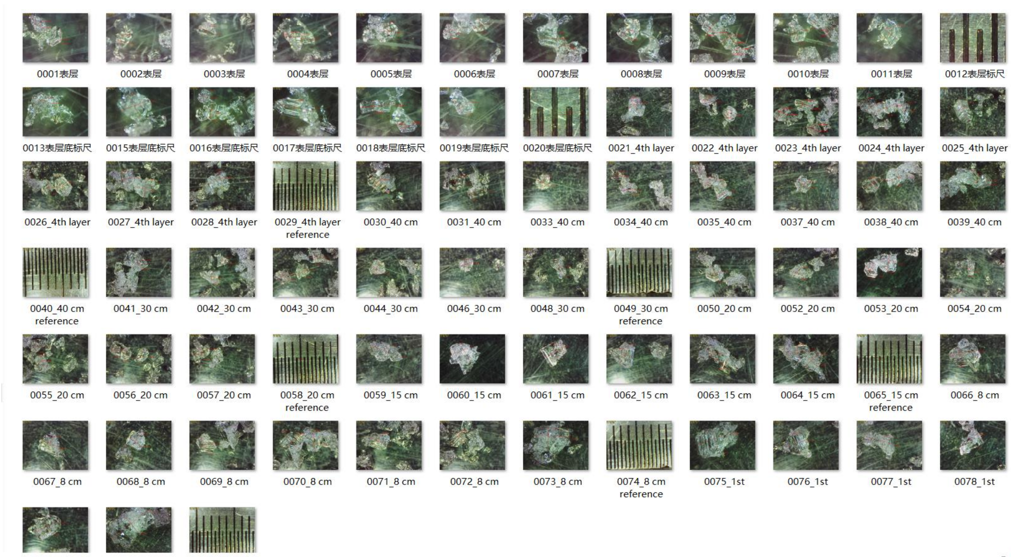

Figure A1: Photos of grains and reference ruler in each layer on February 15, 2016, and in each photo the longest and shortest axis lengths of the chosen grains are labeled.

Table A1. Recorded longest and shortest axis length in Figure A.

Stratigraphy	Thickness (cm)	Shape	Grain size (longest axis * shortest axis)(mm)								
the fifth	3cm	#22	0.595*0.436	0.472*0.471	0.450*0.436	0.615*0.474	0.374*0.314	0.647*0.307	0.656*0.529	0.544*0.519	0.717*0.447
			0.750*0.445	1.056*0.955	0.623*0.378	0.451*0.405	1.397*0.635	1.235*0.327	0.600*0.421	0.633*0.556	0.729*0.423
the fourth	3cm	#37	2.605*2.011	1.850*1.328	1.626*1.554	1.767*1.685	1.718*1.535	2.255*1.296	1.674*1.601	1.542*1.269	3.505*1.440
			3.055*1.774	1.448*1.37	2.461*1.914	2.757*2.115	2.179*2.059	2.393*1.788			
the third	25cm	#27，#31，#37	2.569*1.607	2.073*2.130	2.591*1.414	1.869*1.802	2.067*1.266	1.209*1.106	1.719*1.188	1.648*0.975	1.911*1.582

https://doi.org/10.5194/essd-2022-68
Preprint. Discussion started: 4 March 2022

Open Access Earth System Science Data Discussions

			1.921 *1.710	1.518 *1.067	1.291 *1.147	1.690 *1.551	1.756 *1.398	1.812 *1.263	1.733 *1.672	1.880 *1.518	2.411 *1.220
			2.118 *1.727	1.614 *1.457	1.795 *1.705	2.215 *2.311	1.864 *1.692	1.967 *1.651	2.008 *1.395	1.362 *1.141	1.484 *1.291
the second	12	#33，#34	4.251 *2.266	3.012 *2.65	2.805 *1.995	1.799 *1.415	1.402 *1.195	3.040 *2.073	2.850 *2.095		
			3.900 *2.532	2.420 *2.333	2.515 *2.206	2.044 *2.032	2.506 *2.363	2.894 *2.161	2.413 *1.950	2.494 *1.816	4.929 *3.257
the first	4	#40，#34，#38	4.933 *3.378	3.207 *2.774	3.562 *1.701	2.818 *1.668	3.581 *2.518	6.179 *3.562			

Table A2: One example of record table for snow density observation.

observation date:	20160111	observation	9:03-9:40	weather:	clear	snow depth:	48cm

Snow Folk table

observation height (cm)	liquid water content (%)	snow density (g/cm3)
5	0	0.1923
	0.118	0.1882
	0	0.1882
10	0.461	0.164
	0.46	0.1631
	0.461	0.1361
15	0.123	0.2532
	0	0.2506
	0	0.2417
20	0.24	0.2159
	0.119	0.2155
	0.119	0.2146
25	0.117	0.1977
	0	0.1994
	0	0.1984
30	0	0.1919
	0	0.1966
	0	0.1928
35	0	0.1534
	0	0.1517
	0	0.1472
40	0.325	0.1097
	0	0.1054
	0.107	0.1088
45	0	0.0922
	0	0.0991
	0	0.0928
50		
55		

snow tube table

snow depth (cm)	46.5	47	47.5
snow pressure (g/cm2)	9.1	9	9.5
snow density (g/cm3)	0.1957	0.1915	0.2000

snow shovel table

observation layer (cm)	weight of shovel+snow (g)	weight of shovel (g)	snow density (g/cm3)
0-10	865.04	572.16	0.1953
	858.72	572.16	0.1910
	866.69	572.16	0.1964
10-20	878.58	572.16	0.2043
	887.04	572.16	0.2099
	872.79	572.16	0.2004
20-30	905.34	572.16	0.2221
	903.41	572.16	0.2208
	907.88	572.16	0.2238
30-40	832.75	572.16	0.1737
	838.14	572.16	0.1773
	837.27	572.16	0.1767
40-50			
50-60			

https://doi.org/10.5194/essd-2022-68
Preprint. Discussion started: 4 March 2022

References:

Babaeian, E., Sadeghi, M., Jones, S.B., Montzka, C., Vereecken, H., and Tuller, M.: Ground, Proximal, and Satellite Remote Sensing of Soil Moisture. Reviews of Geophysics, 57(2), 530-616, doi: 10.1029/2018RG000618, 2019.

Barnett, T.P., Adam, J.C., and Lettenmaier, D.P.: Potential impacts of a warming climate on water availability in snow-dominated regions. *Nature, 438*, 303-309, doi: 10.1038/nature04141, 2005.

Brucker, L., Hiemstra, C., Marshall, H.-P., Elder, K., De Roo, R., Mousavi, M., Bliven, F., Peterson, W., Deems, J., Gadomski, P., Gelvin, A., Spaete, L., Barnhart, T., Brandt, T., Burkhart, J., Crawford, C., Datta, T., Erikstrod, H., Glenn, N., Hale, K., Holben, B., Houser, P., Jennings, K., Kelly, R., Kraft, J., Langlois, A., McGrath, D., Merriman, C., Molotch, N., Nolin, A., Polashenski, C., Raleigh, M., Rittger, K., Rodriguez, C., Roy, A., Skiles, M., Small, E., Tedesco, M., Tennant, C., Thompson, A., Tian, L., Uhlmann, Z., Webb, R., Wingo, M., and Ieee: A FIRST OVERVIEW OF SNOWEX GROUND-BASED REMOTE SENSING ACTIVITIES DURING THE WINTER 2016-2017. *2017 Ieee International Geoscience and Remote Sensing Symposium* (pp. 1391-1394), 2017

Che, T., Dai, L.Y., Zheng, X.M., Li, X.F., and Zhao, K.: Estimation of snow depth from passive microwave brightness temperature data in forest regions of northeast China. Remote Sensing of Environment, 183, 334-349, doi: 10.1016/j.rse.2016.06.005, 2016.

Che, T., Li, X., Jin, R., Armstrong, and R., Zhang ,T.J. : Snow depth derived from passive microwave remote-sensing data in China. *Annals of Glaciology, 49*, 145. doi: 10.3189/172756408787814690, 2008.

Chen, T., Pan, J.M., Chang, S.L., Xiong, C., Shi, J.C., Liu, M.Y., Che, T., Wang, L.F., and Liu, H.R. : Validation of the SNTHERM Model Applied for Snow Depth, Grain Size, and Brightness Temperature Simulation at Meteorological Stations in China. *Remote Sensing,* 12, 507, doi: Artn 50710.3390/Rs12030507, 2020.

Cline, D., Elder, K., Davis, B., Hardy, J., Liston, G., Imel, D., Yueh, S., Gasiewski, A., Koh, G., Amstrong, R., and Parsons, M.: An overview of the NASA Cold Land Processes Field Experiment (CLPX-2002). Microwave Remote Sensing of the Atmosphere and Environment Iii, 4894, 361-372. doi: Doi 10.1117/12.467766, 2003.

Cohen, J: Snow cover and climate. Weather, 49, 150-156, 1994.

Dai, L. (2020): Microwave radiometry experiment data in Altay (2015/2016). National Tibetan Plateau Data Center [dataset]. doi: 10.11888/Snow.tpdc.270886, 2020.

Dai, L.Y., Che, T., Wang, J., and Zhang, P. :Snow depth and snow water equivalent estimation from AMSR-E data based on a priori snow characteristics in Xinjiang, China. *Remote Sensing of Environment, 127*, 14-29,. doi: 10.1016/j.rse.2011.08.029, 2012.

Derksen, C., Toose, P., Lemmetyinen, J., Pulliainen, J., Langlois, A., Rutter, N., and Fuller, M.C.: Evaluation of passive microwave brightness temperature simulations and snow water equivalent retrievals through a winter season. *Remote Sensing of Environment, 117*, 236-248, doi: 10.1016/j.rse.2011.09.021, 2012.

Ding, Y.J., Yang, J.P., Wang, S.X., and Chang, Y.P.: A review of the interaction between the cryosphere and atmosphere. Sciences in Cold and Arid Regions, 12 (6): 329-342, doi: 10.3724/SP.J.1226.2020.00329, 2020.

Essery, R.: A factorial snowpack model (FSM 1.0). Geosci. Model Dev. 2015, 8, 3867–3876.

Hirahara,Y., de Rosnay, P., and Arduini, G.: Evaluation of a Microwave Emissivity Module for Snow Covered Area with CMEM in the ECMWF Integrated Forecasting System. Remote Sensing, 12(18), doi: Artn 294610.3390/Rs12182946, 2020.

Immerzeel, W.W., van Beek, L.P.H., and Bierkens, M.F.P.: Climate Change Will Affect the Asian Water Towers. Science, 328(5984), 1382-1385. doi: 10.1126/science.1183188, 2010.

Jiang, L.M., Wang, P., Zhang, L.X., Yang, H., and Yang, J.T.: Improvement of snow depth retrieval for FY3B-MWRI in China. Science China-Earth Sciences, 57, 1278-1292, doi: 10.1007/s11430-013-4798-8, 2014.

Jordan, R.E.: A One-Dimensional Temperature Model for a Snow Cover: Technical Documentation for SNTHERM.89; U.S. Army Cold Regions Research and Engineering Laboratory: Hanover, NH, USA, 1991.

Lehning, M., Bartelt, P., Brown, B., Fierz, C., and Satyawali, P.: A physical SNOWPACK model for the Swiss avalanche warning Part II: Snow microstructure. *Cold Regions Science and Technology, 35*, 147-167, Doi 10.1016/S0165-232x(02)00073-3, 2002.

Lemmetyinen, J., Kontu, A., Pulliainen, J., Vehvilainen, J., Rautiainen, K., Wiesmann, A., Matzler, C., Werner, C., Rott, H., Nagler, T., Schneebeli, M., Proksch, M., Schuttemeyer, D., Kern, M., and Davidson, M.W.J. : Nordic Snow Radar Experiment. Geoscientific Instrumentation Methods and Data Systems, 5, 403-415, doi: 10.5194/gi-5-403-2016, 2016.

Löwe H. and Picard, G. “Microwave scattering coefficient of snow in MEMLS and DMRT-ML revisited: The relevance of sticky hard spheres and tomography-based estimates of stickiness,” Cryosphere, vol. 9, no. 6, pp. 2101–2117, Nov. 2015.

Mortimer, C., Mudryk, L., Derksen, C., Luojus, K., Brown, R., Kelly, R., and Tedesco, M. : Evaluation of long-term Northern Hemisphere snow water equivalent products. Cryosphere, 14(5), 1579-1594, doi: 10.5194/tc-14-1579-2020, 2020.

Naderpour, R., Schwank, M., Matzler, C., Lemmetyinen, J., and Steffen, K.: Snow Density and Ground Permittivity Retrieved From L-Band Radiometry: A Retrieval Sensitivity Analysis. Ieee Journal of Selected Topics in Applied Earth Observations and Remote Sensing, 10(7), 3148-3161, doi: 10.1109/Jstars.2017.2669336, 2017.

Pulliainen, J., Luojus, K., Derksen, C., Mudryk, L., Lemmetyinen, J., Salminen, M., Ikonen, J., Takala, M., Cohen, J., Smolander, T., and Norberg, J.: Patterns and trends of Northern Hemisphere snow mass from 1980 to 2018. Nature, 581(7808), 294-298. doi: 10.1038/s41586-020-2258-0, 2020.

Roy, A., Picard, G., Royer, A., Montpetit, B., Dupont, F., Langlois, A., Derksen, C., and Champollion, N.: Brightness Temperature Simulations of the Canadian Seasonal Snowpack Driven by Measurements of the Snow Specific Surface Area. *Ieee Transactions on Geoscience and Remote Sensing, 51*, 4692-4704, doi: 10.1109/Tgrs.2012.2235842, 2013.

Roy, A., Picard, G., Royer, A., Montpetit, B., Dupont, F., Langlois, A., Derksen, C., and Champollion, N.: Brightness Temperature Simulations of the Canadian Seasonal Snowpack Driven by Measurements of the Snow Specific Surface Area, IEEE T. Geosci. Remote, 51, 4692–4704, doi:10.1109/TGRS.2012.2235842, 2013

Tedesco, M., Narvekar, P.S.: Assessment of the NASA AMSR-E SWE Product. Ieee Journal of Selected Topics in Applied Earth Observations and Remote Sensing, 3, 141-159, doi: 10.1109/Jstars.2010.2040462, 2010.

Vionnet, V., Brun, E., Morin, S., Boone, A., Faroux, S., Le Moigne, P., Martin, E., and Willemet, J.M.: The detailed snowpack scheme Crocus and its implementation in SURFEX v7.2. *Geoscientific Model*

https://doi.org/10.5194/essd-2022-68
Preprint. Discussion started: 4 March 2022

Development, 5, 773-791, doi: 10.5194/gmd-5-773-2012, 2012.

Xiao, L., Che, T., and Dai, L.Y.: Evaluation of Remote Sensing and Reanalysis Snow Depth Datasets over the Northern Hemisphere during 1980-2016. Remote Sensing, 12(19), doi: Artn 325310.3390/Rs12193253, 2020.

Yang, Z.L., Dickinson, R.E., Robock, A., and Vinnikov, K.Y. : Validation of the snow submodel of the biosphere-atmosphere transfer scheme with Russian snow cover and meteorological observational data. *Journal of Climate, 10*, 353-373, doi: 10.1175/1520-0442(1997)010<0353:Votsso>2.0.Co;2, 1997.